A posteriori inclusion of parton density functions in NLO QCD final state calculations

Pavel Starovoitov

DESY

September 30, 2014

Proton-proton collision

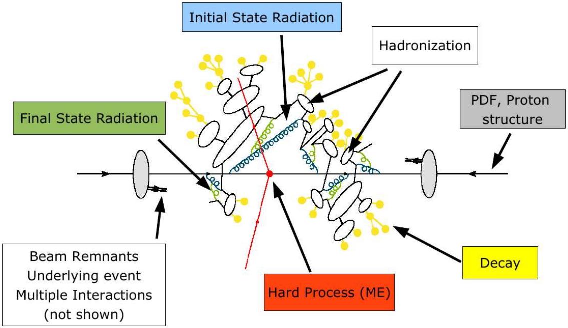

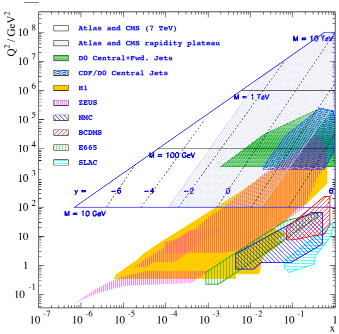

- hard scattering can be calculated to NLO(NNLO) precision
- description of showers and non-perturbative effects comes from MC
- PDFs and strong coupling are determined from precision data (LEP, HERA, TEVATRON, . . .).

NLO QCD cross section

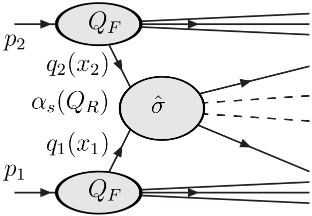

$$\frac{d\sigma}{dX} \sim \sum_{(i,j,p)} \int d\Gamma \alpha_s^p(Q_R^2)\, q_i(x_1, Q_F^2) q_j(x_2, Q_F^2)\, \frac{d\hat{\sigma}^{ij}_{(p)}}{dX}(x_1, x_2, Q_F^2, Q_R^2;\ S)$$

- Coupling and parton density functions are non-perturbative inputs to calculation (extracted from data)
- Perturbative coefficients are essentially independent from PDF functions due to factorization theorem

Calculating NLO cross-sections takes a long time ($\sim$ *days*)

$\Longrightarrow$ we can split calculation into two parts

APPLGRID method

Eur.Phys.J.C66:503-524,2010.

- Step 1 (long run): Collect perturbative weights to grids .
  - binning
  - interpolation
  - initial flavours decomposition : $13 \times 13 \to \mathcal{L}$ ($\mathcal{L} \sim 10$)

$$\frac{d\hat{\sigma}^{ij}_{(p)}}{dX}(x_1, x_2, Q_F^2, Q_R^2;\ S) \xrightarrow{3D-grid} w^{(p)(l)}(x_1^m, x_2^n, Q^{2^k})\ (Q_R^2 \equiv Q_F^2)$$

- Step 2 ($\sim$ 10–100 ms): Convolute grid with PDF's .
  - integral $\to$ sum
  - any coupling, PDF

Details of the method (I)

Interpolation

- user defined interpolation orders $n_y, \quad n_\tau$

$$f(x,Q^2) = \sum_{i=0}^{n_y} \sum_{\iota=0}^{n_\tau} f_{k+i,\kappa+\iota}\; I_i^{(n)}\left(\frac{y(x)}{\delta y} - k\right)\; I_\iota^{(n')}\left(\frac{\tau(Q^2)}{\delta\tau} - \kappa\right)$$

Subprocess decomposition

$13 \times 13 \to \mathcal{L}$ due to the symmetries of the ME weights

$$\sum_{m,n} \nu_{mn}^{(l)}\, f_{m/H_1}\left(x_1, Q^2\right) f_{n/H_2}\left(x_2, Q^2\right) \equiv F^{(l)}\left(x_1, x_2, Q^2\right),$$

“generalised“ PDFs depend on the process and the perturbative order

Details of the method (II)

Phasespace optimisation

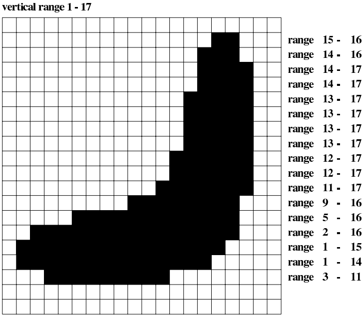

User just defines max/min possible values of x, Q^2. The optimisation procedure finds appropriate limits for each subprocess/order/observable bin.

$\longleftarrow$ $x_1 x_2$−phasespace

Final result

$$\frac{d\sigma}{dX} = \sum_p \sum_{l=0}^{L} \sum_{m,n,k} w_{m,n,k}^{(p)(l)} \left(\frac{\alpha_s(Q_k^2)}{2\pi} \right)^{p_l} F^{(l)}\left(x_{1\,m}, x_{2\,n}, Q_k^2\right)$$

Scale dependence I

Having the weights $w^{(p)(l)}_{m,n,k}$ determined separately order by order in α_s, it is straightforward to vary the renormalisation μ_R and factorisation μ_F scales a posteriori.
We assume scales to be equal

$$\mu_R = \mu_F = Q$$

in the original calculation.
Let we introduce ξ_R and ξ_F corresponding to the factors by which one varies μ_R and μ_F respectively,

$$\mu_R = \xi_R \times Q$$
$$\mu_F = \xi_F \times Q$$

Scale dependence II

Then for arbitrary ξ_R and ξ_F we may write:

$$\frac{d\sigma}{dX}(\xi_R, \xi_F) = \sum_{l=0}^{L} \sum_{m} \sum_{n} \sum_{k} \Bigg\{ \left(\frac{\alpha_s\left(\xi_R^2 {Q^2}_k\right)}{2\pi} \right)^{p_{\mathrm{LO}}}$$

$$\times W_{m,n,k}^{(p_{\mathrm{LO}})(l)} F^{(l)}\left(x_{1\,m}, x_{1\,n}, \xi_F^2 {Q^2}_k\right) + \left(\frac{\alpha_s\left(\xi_R^2 {Q^2}_k\right)}{2\pi} \right)^{p_{\mathrm{NLO}}}$$

$$\times \Bigg[\left(W_{m,n,k}^{(p_{\mathrm{NLO}})(l)} + 2\pi\beta_0 p_{\mathrm{LO}} \ln \xi_R^2 \, W_{m,n,k}^{(p_{\mathrm{LO}})(l)} \right) F^{(l)}\left(x_{1\,m}, x_{2\,n}, \xi_F^2 {Q^2}_k\right)$$

$$- \ln \xi_F^2 \, W_{m,n,k}^{(p_{\mathrm{LO}})(l)}$$

$$\times \left(F_{q_1 \to P_0 \otimes q_1}^{(l)}\left(x_{1\,m}, x_{2\,n}, \xi_F^2 {Q^2}_k\right) + F_{q_2 \to P_0 \otimes q_2}^{(l)}\left(x_{1\,m}, x_{2\,n}, \xi_F^2 {Q^2}_k\right) \right) \Bigg] \Bigg\},$$

where $F_{q_1 \to P_0 \otimes q_1}^{(l)}$ is calculated as $F^{(l)}$, but with q_1 replaced with $P_0 \otimes q_1$ (LO splitting function convoluted with PDF), and analogously for $F_{q_2 \to P_0 \otimes q_2}^{(l)}$.

Interface to cross section calculators

- NLOJET++ : Jet production in $pp(\bar{p})-$ and $ep-$ collisions.
  - $2 \to 2$ and $2 \to 3$ at NLO; $2 \to 4$ at LO www.desy.de/~znagy/Site/NLOJet++.htm.
- MCFM : parton-level NLO QCD cross sections calculator for various femtobarn-level processes at hadron-hadron colliders.
  - $V, V + nJet, V + b\bar{b}, VV, Q\bar{Q}, \ldots (\sim \mathcal{O}(300))$ mcfm.fnal.gov/
- SHERPA : Simulation of High-Energy Reactions of PArticles in lepton-lepton, lepton-photon, photon-photon, lepton-hadron and hadron-hadron collisions.
  - A huge amount of scattering processes sherpa.hepforge.org.
- aMC@NLO : A framework for the computation of hard events at the NLO or LO, to be subsequently showered (infrared-safe observables at the NLO or LO).
  - Matrix elements calculations from Madgraph 5 amcatnlo.web.cern.ch/amcatnlo/; madgraph.phys.ucl.ac.be/.
- DYNNLO : NNLO calculation of Drell-Yan processes at hadron colliders theory.fi.infn.it/grazzini/dy.html

APPLGRID subprocesses for $W^{\pm}$ production (I)

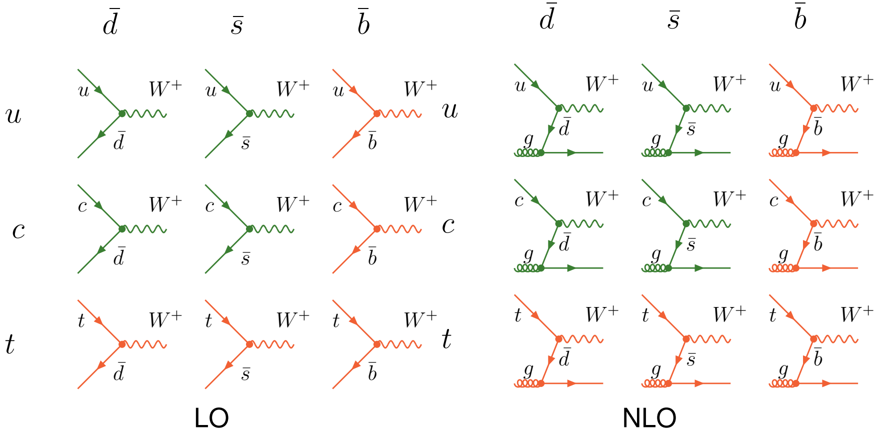

APPLGRID subprocesses for $W^{\pm}$ production (II)

The weights for W^{+}-production can be organized in six possible initial state combinations (calculated using MCFM)

$$\bar{D}U: \quad F^{(0)}\left(x_1, x_2, Q^2\right) = \sum_{j=1,3,5} f_{-j/H_1}\left(x_1\right) \sum_{i=2,4,6} f_{i/H_2}\left(x_2\right) V_{ij}^2$$

$$U\bar{D}: \quad F^{(1)}\left(x_1, x_2, Q^2\right) = \sum_{i=2,4,6} f_{i/H_1}\left(x_1\right) \sum_{j=1,3,5} f_{-j/H_2}\left(x_2\right) V_{ij}^2$$

$$Ug: \quad F^{(3)}\left(x_1, x_2, Q^2\right) = \sum_{i=2,4,6} f_{i/H_1}\left(x_1\right) \left(V_{id}^2 + V_{is}^2 + V_{ib}^2\right) f_{0/H_2}\left(x_2\right)$$

$$gU: \quad F^{(5)}\left(x_1, x_2, Q^2\right) = \sum_{i=2,4,6} f_{0/H_1}\left(x_1\right) \left(V_{id}^2 + V_{is}^2 + V_{ib}^2\right) f_{i/H_2}\left(x_2\right)$$

$$g\bar{D}: \quad F^{(4)}\left(x_1, x_2, Q^2\right) = \sum_{i=1,3,5} f_{0/H_1}\left(x_1\right) \left(V_{iu}^2 + V_{ic}^2 + V_{it}^2\right) f_{-i/H_2}\left(x_2\right)$$

$$\bar{D}g: \quad F^{(2)}\left(x_1, x_2, Q^2\right) = \sum_{i=1,3,5} f_{-i/H_1}\left(x_1\right) \left(V_{iu}^2 + V_{ic}^2 + V_{it}^2\right) f_{0/H_2}\left(x_2\right)$$

We separate $u\bar{d}$ from $\bar{d}u$ in order to get the right rapidity distribution for the electron,

because of the chiral nature of the $W^{\pm}$ couplings

$W^{\pm}$ production theory uncertainties

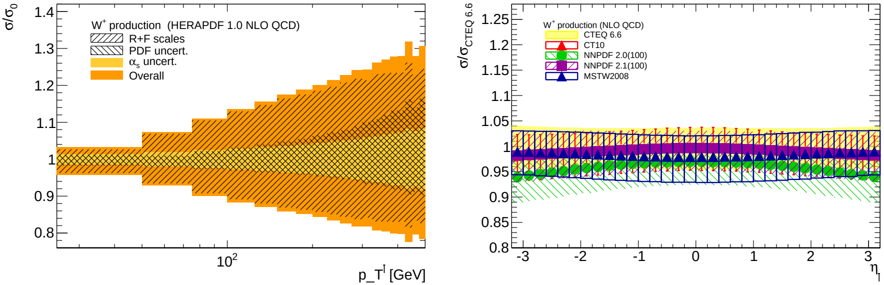

positron p_T

- the scale uncertainty is the dominant one
- theoretical uncertainy decreases when adding more data (and more precise data) to pdf fits
- different PDFs predict slightly different normalisation and shape

Use-case

Determination of the strange-quark density from measurements of W and Z cross-sections

Phys.Rev.Lett. 109 (2012) 012001

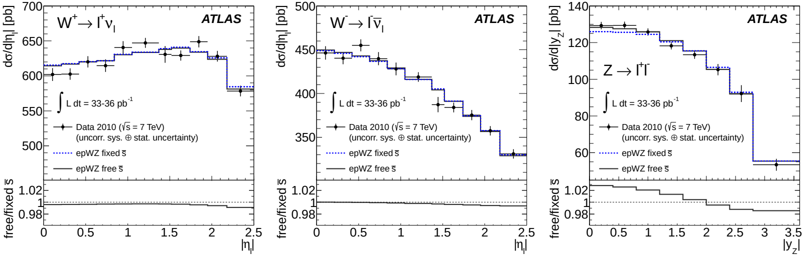

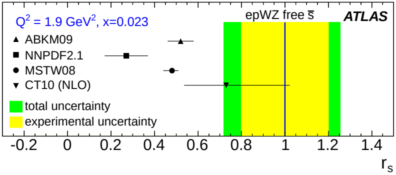

The W/Z measurements introduce a sensitivity to the strange quark density at $x \sim 0.1$. The ratio of the strange to the down sea quark density is found to be $r_s = 1.00^{+0.25}_{-0.28}$ at $x = 0.023$ and the initial scale $Q_0^2 = 1.9\ \mathrm{GeV}^2$

APPLGRID subprocesses for jet production

perturbative coefficients for jet production could be organised in seven subprocesses (calculated using NLOJET++)

$$\begin{aligned}
\mathrm{gg}: \quad F^{(0)}(x_1,x_2;Q^2) &= G_1(x_1)G_2(x_2) \\
\mathrm{qg}: \quad F^{(1)}(x_1,x_2;Q^2) &= \left(Q_1(x_1)+\overline{Q}_1(x_1)\right)G_2(x_2) \\
\mathrm{gq}: \quad F^{(2)}(x_1,x_2;Q^2) &= G_1(x_1)\left(Q_2(x_2)+\overline{Q}_2(x_2)\right) \\
\mathrm{qq}': \quad F^{(3)}(x_1,x_2;Q^2) &= Q_1(x_1)Q_2(x_2)+\overline{Q}_1(x_1)\overline{Q}_2(x_2)-D(x_1,x_2) \\
\mathrm{qq}: \quad F^{(4)}(x_1,x_2;Q^2) &= D(x_1,x_2) \\
\mathrm{q\bar{q}}: \quad F^{(5)}(x_1,x_2;Q^2) &= \overline{D}(x_1,x_2) \\
\mathrm{q\bar{q}}': \quad F^{(6)}(x_1,x_2;Q^2) &= Q_1(x_1)\overline{Q}_2(x_2)+\overline{Q}_1(x_1)Q_2(x_2)-\overline{D}(x_1,x_2)
\end{aligned}$$

$$D(x_1,x_2)=\sum_{\substack{i=-6\\ i\neq 0}}^{6} f_{i/H_1}(x_1,Q^2)f_{i/H_2}(x_2,Q^2), \quad \overline{D}(x_1,x_2)=\sum_{\substack{i=-6\\ i\neq 0}}^{6} f_{i/H_1}(x_1,Q^2)f_{-i/H_2}(x_2,Q^2)$$

Inclusive jets in the $|y| < 0.3$

- the gluon-gluon subprocess falls quickly from $\sim 60\%$ to $\sim 5\%$ for jet $p_{\mathrm{T}} \geq 1.5$ TeV
- The quark-gluon scattering grows from 35% to 50% for jet $p_{\mathrm{T}} \sim$ 400–500 GeVand it slightly decreases to 30% at high p_{T}.
- the quark-quark subprocesses are very small at low jet p_T, but it is dominant at high p_T.

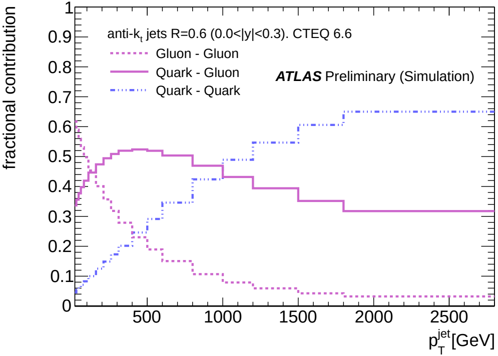

New jet data

- New precise jet data (inclusve, dijet, three-jet) are available.
- We have tools to interpret them!

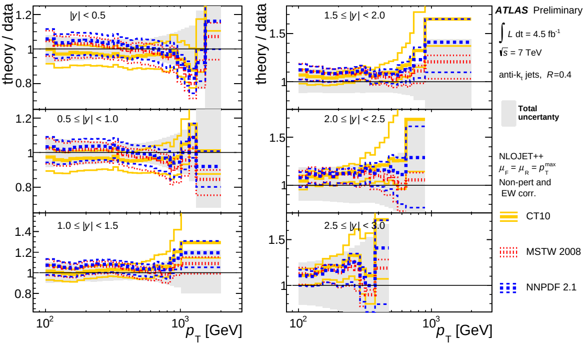

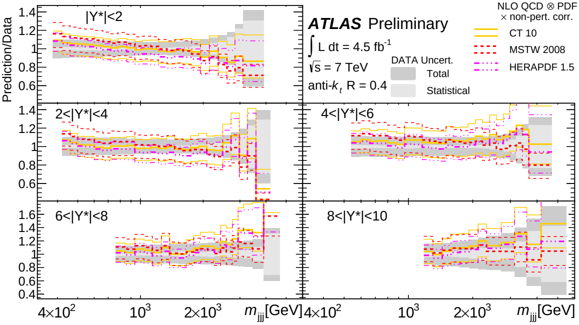

APPLGRID accuracy.

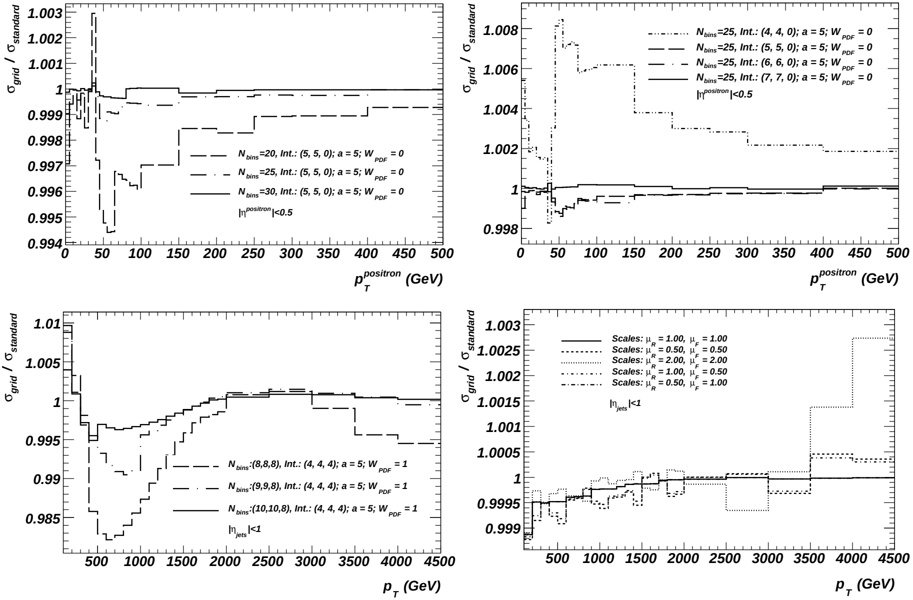

APPLGRID summary

- APPLGrid is an open project, source code is available as HEPforge package:https://projects.hepforge.org/applgrid
- Calculations are performed via the interface to Monte Carlo calculators
    - jet production
    - $W^{\pm}, Z^{0}, \gamma$
    - $W^{\pm}$+charm, $W^{\pm}/Z^{0}/\gamma$+jet
    - $Q\bar{Q}(c\bar{c}, b\bar{b}, t\bar{t})$
    - $t\bar{t} \rightarrow b\ell^{+}\nu_{\ell} + b\ell^{-}\bar{\nu_{\ell}}$, $t\bar{t} \rightarrow b\ell^{+}\nu_{\ell} + bq\bar{q}$, $t\bar{t} \rightarrow bq\bar{q} + b\ell^{-}\bar{\nu_{\ell}}$
    - many others via non-optimal flavour decomposition (*i.e.* 121 initial channels)
- Efficient a posteriori evaluation of uncertainties from renormalisation and factorisation scale variations, strong coupling measurement and PDFs error sets.
- A posteriori centre-of-mass energy rescaling
- Allows rigorous inclusion of NLO cross-sections in a fit.

PDF fit : HERA I + ATLAS jets

Jet cross sections at $\sqrt{s} = 2.76$ and $\sqrt{s} = 7\,\mathrm{TeV}$ are fitted simultaneously, together with HERA I data

HERAPDF-inspired ansatz

$$
\begin{aligned}
xu_v(x) &= A_{u_v} x^{B_{u_v}} (1-x)^{C_{u_v}} \\
&\quad \times (1 + E_{u_v} x^2), \\
xd_v(x) &= A_{d_v} x^{B_{d_v}} (1-x)^{C_{d_v}}, \\
x\bar{U}(x) &= A_{\bar{U}} x^{B_{\bar{U}}} (1-x)^{C_{\bar{U}}}, \\
x\bar{D}(x) &= A_{\bar{D}} x^{B_{\bar{D}}} (1-x)^{C_{\bar{D}}}, \\
xg(x) &= A_g x^{B_g} (1-x)^{C_g} \\
&\quad - A'_g x^{B'_g} (1-x)^{C'_g}
\end{aligned}
$$

Here $\bar{U} = \bar{u}$ whereas $\bar{D} = \bar{d} + \bar{s}$. The parameters A_{u_v} and A_{d_v} are fixed using the quark counting rule and A_g using the momentum sum rule. The normalisation and slope parameters, A and B, of $\bar{u}$ and $\bar{d}$ are set equal such that $x\bar{u} = x\bar{d}$ at $x \to 0$.

- consistent treatment of JES systematics correlations between two ATLAS jet datasets
- $\alpha_S(M_Z) = 0.1176$
- $p_T^{\min}(jet) = 45\,\mathrm{GeV}$ (ATLAS)
- strange fraction $f_s = 0.31$
- starting scale $Q_0^2 = 1.9\,\mathrm{GeV}^2$
- $m_c = 1.4\,\mathrm{GeV}$; $m_b = 4.75\,\mathrm{GeV}$
- $Q^2_{\min} = 3.5\,\mathrm{GeV}^2$ (HERA)
- flexible form of gluon distribution with $C'_g = 25$

In total 13 free parameters to describe the parton densities

PDF constraints: Jets + APPLGRID

- The gluon momentum distribution tends to be harder after the inclusion of the jet data
- PDF sensitivity: different beam energies probe different x, Q^2 for the same η and p_{T} bins

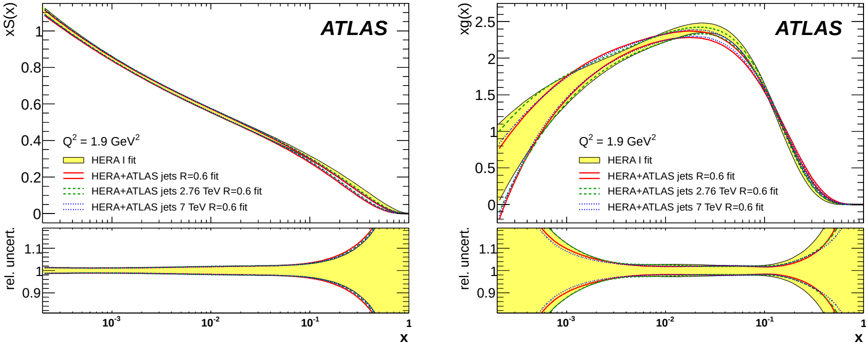

- Very good fit quality is found for both radius parameters
- Shifts of systematics are typically smaller than 0.5σ
- very similar results for fits with $R = 0.4$ and $R = 0.6$ jets

Strong coupling determination using jet data: Introduction

Eur.Phys.J. C72 (2012) 2041

- Input :
  - unfolded double-differential ATLAS inclusive jet cross section data at 7 TeV collisions.
  - NLO jet cross section (APPLGRID) corrected for NP effects
- Method :
  - The measured cross section in each (p_{T}, y) bin is mapped to α_S value.
  - All the experimental uncertainties of cross sections, together with their bin-to-bin correlations, are propagated to the determined α_S values, using pseudo-experiments (toys).
- Result : weighted average across all bins

Strong coupling determination using jet data: Distributions

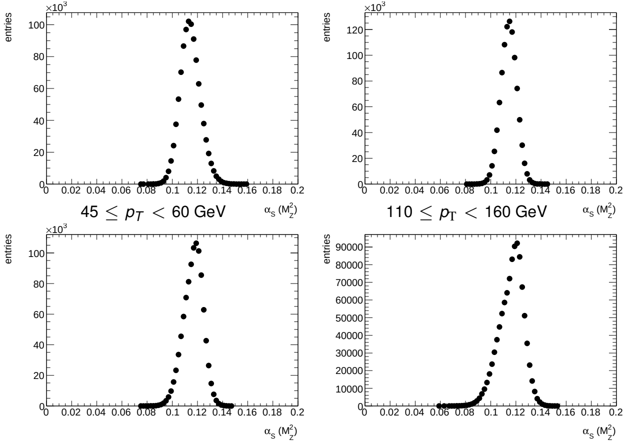

$45 \leq p_T < 60$ GeV

$110 \leq p_T < 160$ GeV

$310 \leq p_T < 400$ GeV

$500 \leq p_T < 600$ GeV

Examples of distributions of $\alpha_s(M_Z)$, as obtained from 10^6 pseudo-experiments, for anti-k_T jets with R=0.6, in the central rapidity region ($0 \leq |y| < 0.3$), in several p_T bins.

Strong coupling determination using jet data: Results in rapidity bins

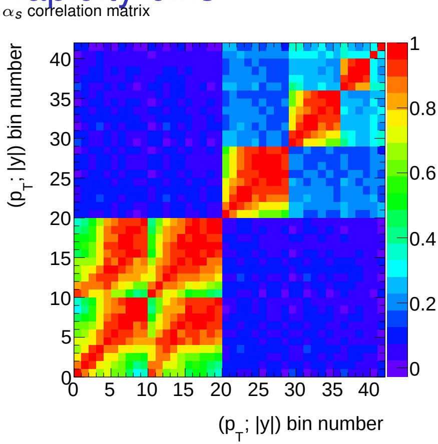

$$\alpha_s(M_Z)^{\mathrm{WA}}(|y|_1) = 0.1155^{+0.0067}_{-0.0069},$$
$$\alpha_s(M_Z)^{\mathrm{WA}}(|y|_2) = 0.1167^{+0.0073}_{-0.0077},$$
$$\alpha_s(M_Z)^{\mathrm{WA}}(|y|_3) = 0.1147^{+0.0075}_{-0.0079},$$
$$\alpha_s(M_Z)^{\mathrm{WA}}(|y|_4) = 0.1145^{+0.0076}_{-0.0080},$$
$$\alpha_s(M_Z)^{\mathrm{WA}}(|y|_5) = 0.1147^{+0.0072}_{-0.0077},$$
$$\alpha_s(M_Z)^{\mathrm{WA}}(|y|_6) = 0.1155^{+0.0085}_{-0.0108},$$
$$\alpha_s(M_Z)^{\mathrm{WA}}(|y|_7) = 0.1000^{+0.0098}_{-0.0080}.$$

The precision of the average in each $|y|$ bin is similar to the precision of the values obtained in the input p_T bins. This is due to the strong correlations between (and the similar size of) the uncertainties in the p_T bins used for the average inside a given $|y|$ bin.

Strong coupling determination using jet data: Result

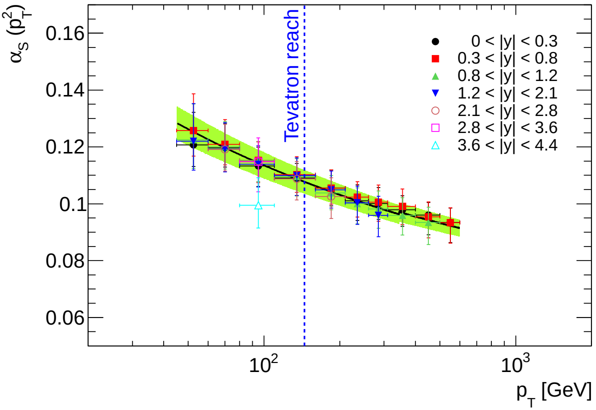

$$\alpha_S(M_Z^2) = 0.1151 \pm 0.0001\,(\text{stat.}) \pm 0.0047\,(\text{exp. syst.}) \pm 0.0014\,(p_T\text{ range})$$
$$\pm 0.0060\,(\text{jet size})^{+0.0044}_{-0.0011}\,(\text{scale})^{+0.0022}_{-0.0015}\,(\text{PDF choice})$$
$$\pm 0.0010\,(\text{PDF eig.})^{+0.0009}_{-0.0034}\,(\text{NP corrections}),$$

Summary

Precision measurements test of QCD can improve knowledge of proton parton density functions and strong coupling constant and facilitate discoveries at LHC.

- APPLGrid is an open project, complete source code is available as HEPforge package:https://projects.hepforge.org/applgrid
- A posteriori evaluation of uncertainties from renormalisation and factorisation scale variations, strong coupling measurement and PDFs error sets in a very short time
- Allows rigorous inclusion of jet and electroweak cross sections in PDF fit.
- Other functionality, such as a posteriori $\sqrt{S}$ rescaling
- A list of QCD and electroweak processes can be studied
  - Jet production cross sections studied using NLOJET++
  - Electroweak observables included using MCFM
  - Many other processes via SHERPA, aMC@NLO

BACK-UP

APPLGRID interface to MCFM.

- MCFM : parton-level NLO QCD cross sections calculator for various femtobarn-level processes at hadron-hadron colliders.
  - V, $V + nJet$, $V + b\bar{b}$, VV, $Q\bar{Q}$,... ($\sim \mathcal{O}(300)$) http://mcfm.fnal.gov/
- Standard analysis :
  - at the end of each event MCFM provides the event record and the weight.
  - user routine (User/nplotter.f): calculates observable(s), applies cuts, fills weight
- APPLGRID is interfaced via common block
  - kinematics : $x_1, x_2, Q, ...$; dynamics :order, weights[]
  - C++ wrapper :
    - ⋆ reads event record, calculates observable $\mathcal{O}$, fills the grid gridObject $\rightarrow$ fillMCFM($\mathcal{O}$);
    - ⋆ fillMCFM(...) reads common block , performs subprocess decomposition, fills the weights

APPLGRID subprocesses for Z^0 production

We can introduce 12 sub-processes in Z production (calculated using MCFM)

$$
\begin{aligned}
U\bar{U}: &\quad F^{(0)}(x_1, x_2, Q^2) = U_{12}(x_1, x_2)\\
D\bar{D}: &\quad F^{(1)}(x_1, x_2, Q^2) = D_{12}(x_1, x_2)\\
\bar{U}U: &\quad F^{(2)}(x_1, x_2, Q^2) = U_{21}(x_1, x_2)\\
\bar{D}D: &\quad F^{(3)}(x_1, x_2, Q^2) = D_{21}(x_1, x_2)\\
gU: &\quad F^{(4)}(x_1, x_2, Q^2) = G_1(x_1)U_2(x_2)\\
g\bar{U}: &\quad F^{(5)}(x_1, x_2, Q^2) = G_1(x_1)\overline{U}_2(x_2)\\
gD: &\quad F^{(6)}(x_1, x_2, Q^2) = G_1(x_1)D_2(x_2)\\
g\bar{D}: &\quad F^{(7)}(x_1, x_2, Q^2) = G_1(x_1)\overline{D}_2(x_2)\\
Ug: &\quad F^{(8)}(x_1, x_2, Q^2) = U_1(x_1)G_2(x_2)\\
\bar{U}g: &\quad F^{(9)}(x_1, x_2, Q^2) = \overline{U}_1(x_1)G_2(x_2)\\
Dg: &\quad F^{(10)}(x_1, x_2, Q^2) = D_1(x_1)G_2(x_2)\\
\bar{D}g: &\quad F^{(11)}(x_1, x_2, Q^2) = \overline{D}_1(x_1)G_2(x_2)
\end{aligned}
$$

We separate $u\bar{u}$ from $\bar{u}u$ contributions to include γ/Z interference

APPLGRID subprocesses for Z^0 production II

Use is made of the generalised PDFs defined as:

$$U_H(x) = \sum_{i=2,4,6} f_{i/H}\left(x, Q^2\right), \qquad \overline{U}_H(x) = \sum_{i=2,4,6} f_{-i/H}\left(x, Q^2\right),$$

$$D_H(x) = \sum_{i=1,3,5} f_{i/H}\left(x, Q^2\right), \qquad \overline{D}_H(x) = \sum_{i=1,3,5} f_{-i/H}\left(x, Q^2\right),$$

$$U_{12}(x_1, x_2) = \sum_{i=2,4,6} f_{i/H_1}\left(x_1, Q^2\right) f_{-i/H_2}\left(x_2, Q^2\right),$$

$$D_{12}(x_1, x_2) = \sum_{i=1,3,5} f_{i/H_1}\left(x_1, Q^2\right) f_{-i/H_2}\left(x_2, Q^2\right),$$

$$U_{21}(x_1, x_2) = \sum_{i=2,4,6} f_{-i/H_1}\left(x_1, Q^2\right) f_{i/H_2}\left(x_2, Q^2\right),$$

$$D_{21}(x_1, x_2) = \sum_{i=1,3,5} f_{-i/H_1}\left(x_1, Q^2\right) f_{i/H_2}\left(x_2, Q^2\right),$$

Z^0 production theory uncertainties

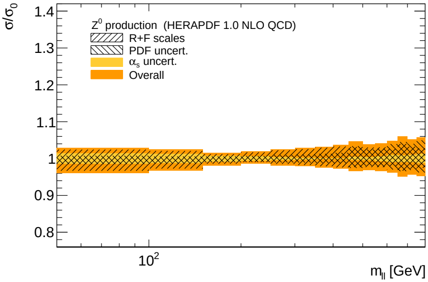

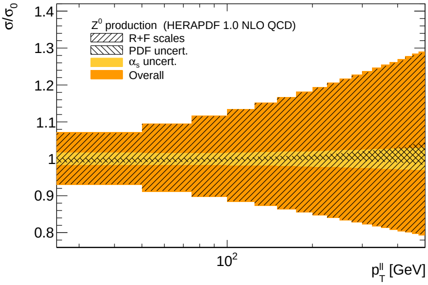

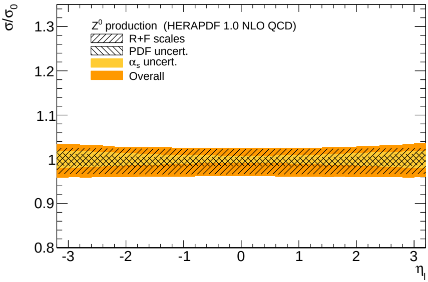

Z^0 production lepton rapidity. PDF comparison

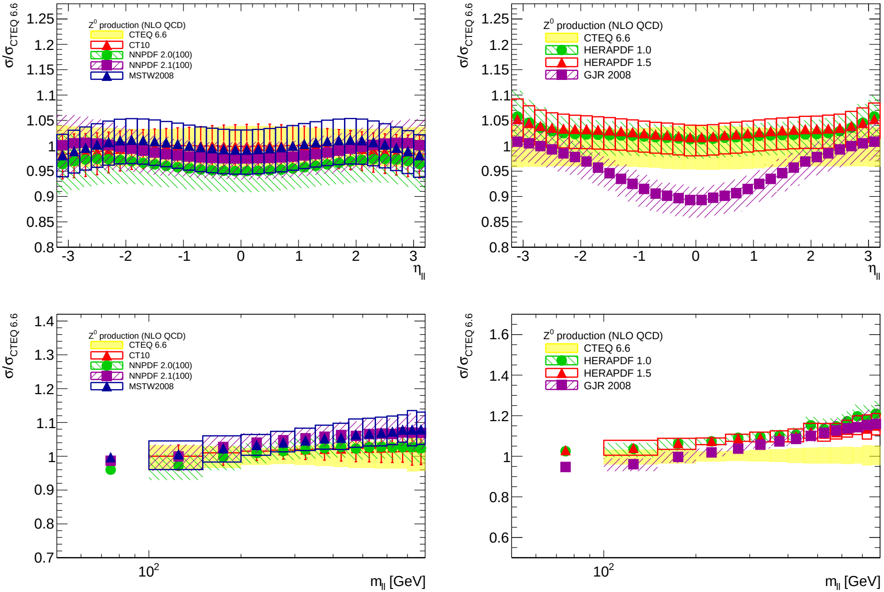

Z^0 production Total cross section

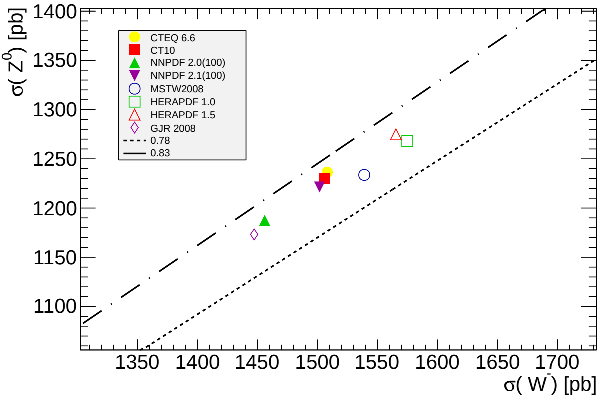

different PDFs predict 10% different total cross section, but they all predict quite the same ratio.

APPLGRID subprocesses for $Q\overline{Q}$ production

The weights for $Q\bar{Q}$-production can be organized in six possible initial state combinations (calculated using MCFM)

$$
\begin{aligned}
\mathrm{gg}: &\quad F^{(0)}(x_1, x_2; Q^2) = G_1(x_1)G_2(x_2) \\
\mathrm{qg}: &\quad F^{(1)}(x_1, x_2; Q^2) = Q_1(x_1)G_2(x_2) \\
\mathrm{gq}: &\quad F^{(2)}(x_1, x_2; Q^2) = G_1(x_1)Q_2(x_2) \\
\bar{\mathrm{q}}\mathrm{g}: &\quad F^{(3)}(x_1, x_2; Q^2) = \bar{Q}_1(x_1)G_2(x_2) \\
\mathrm{g}\bar{\mathrm{q}}: &\quad F^{(4)}(x_1, x_2; Q^2) = G_1(x_1)\bar{Q}_2(x_2) \\
\mathrm{q}\bar{\mathrm{q}}: &\quad F^{(5)}(x_1, x_2; Q^2) = D_{12}(x_1, x_2) \\
\bar{\mathrm{q}}\mathrm{q}: &\quad F^{(6)}(x_1, x_2; Q^2) = \bar{D}_{12}(x_1, x_2)
\end{aligned}
$$

number of quark flavours : $3(c\bar{c})$, $4(b\bar{b})$, $5(t\bar{t})$

$Q\overline{Q}$ production theory uncertainties

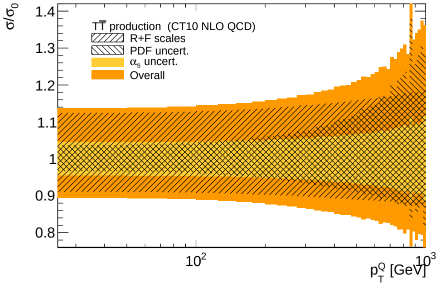

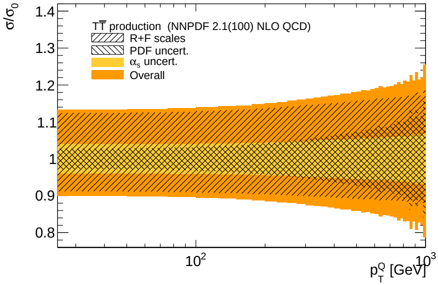

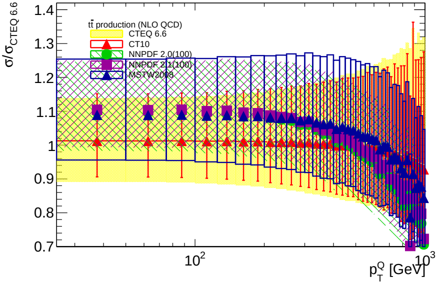

top p_T

- different shape and normalisation
- top differential measurements will provide constraints to PDFs

$Q\overline{Q}$ production PDF comparison

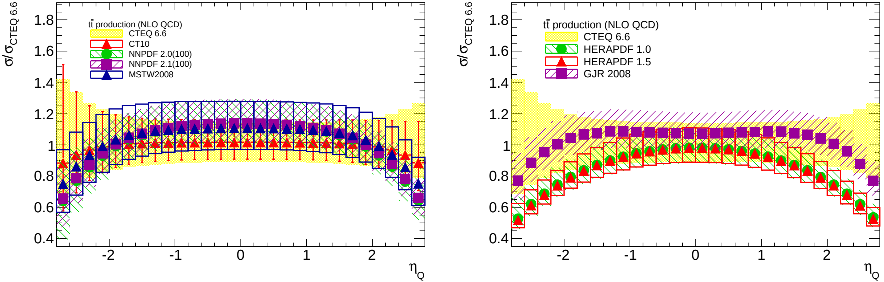

top rapidity

- different PDFs predict different shape

NLOJET++

- input functions
  *void psinput(phasespace_hhc *ps, double& s)* : external phase space generator (if needed), energy [GeV] in C.M.S.

  void inputfunc(unsigned int& nj, unsigned int& nu, unsigned int& nd) : number of parton in final state at LO, number of UP(DOWN) quark flavors
- user class
  class UserHHC : public user1d_hhc {
  public:
  UserHHC(); ∼*UserHHC();*
  void initfunc(unsigned int);
  void userfunc(const event_hhc&, const amplitude_hhc&);
  . . . }
- *UserHHC* :: *userfunc*(. . .) (called every event)
  - *partons* $\xrightarrow{FastJet}$ *jets*
  - event selection
  - *gridObject* → *fill*(. . .)

α_S determination

Eur.Phys.J. C72 (2012) 2041

- Input :
  - unfolded double-differential ATLAS inclusive jet cross section data at 7 TeV collisions.
  - NLO jet cross section corrected for NP effects
- Method :
  - The measured cross section in each (p_T, y) bin is mapped to α_S value.
  - All the experimental uncertainties of cross sections, together with their bin-to-bin correlations, are propagated to the determined α_S values, using pseudo-experiments (toys).
- Result : weighted average across all bins

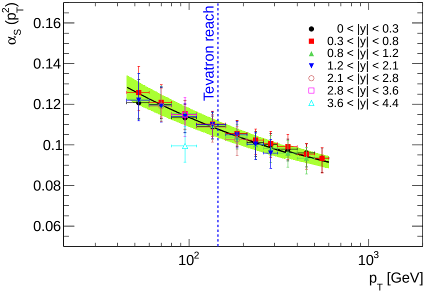

$$\alpha_S(M_Z^2) = 0.1151 \pm 0.0001\,(\text{stat.}) \pm 0.0047\,(\text{exp. syst.}) \pm 0.0014\,(p_T\text{ range}) \pm 0.0060\,(\text{jet size})$$
$$^{+0.0044}_{-0.0011}\,(\text{scale})^{+0.0022}_{-0.0015}\,(\text{PDF choice}) \pm 0.0010\,(\text{PDF eig.})^{+0.0009}_{-0.0034}\,(\text{NP corrections}),$$